Adsorption of aflatoxin B1 to corn by-products

Liu, Yue, Xia, Lei, Galani Yamdeu, Joseph, Gong, Yun Yun and Orfila, Caroline

Yue Liu, Lei Xia, Joseph Hubert Galani Yamdeu, Yun Yun Gong, Caroline Orfila,

Adsorption of aflatoxin B1 to corn by-products,

Food Chemistry,

Volume 440,

2024,

138212,

ISSN 0308-8146,

https://doi.org/10.1016/j.foodchem.2023.138212.

Journal Pre-proofs

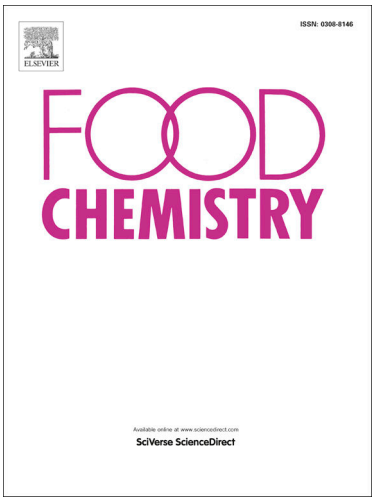

Adsorption of aflatoxin B_1 to corn by-products

Yue Liu, Lei Xia, Joseph Hubert Galani Yamdeu, Yun Yun Gong, Caroline Orfila

PII: S0308-8146(23)02830-3
DOI: https://doi.org/10.1016/j.foodchem.2023.138212
Reference: FOCH 138212

To appear in: *Food Chemistry*

Received Date: 16 September 2023
Revised Date: 6 December 2023
Accepted Date: 12 December 2023

Please cite this article as: Liu, Y., Xia, L., Hubert Galani Yamdeu, J., Yun Gong, Y., Orfila, C., Adsorption of aflatoxin B_1 to corn by-products, *Food Chemistry* (2023), doi: https://doi.org/10.1016/j.foodchem.2023.138212

Adsorption of aflatoxin B_1 to corn by-products

Yue Liu[1,2*], Lei Xia[2], Joseph Hubert Galani Yamdeu[2,3], Yun Yun Gong[2], Caroline Orfila[2†]

1 College of Ocean Food and Biological Engineering, Jimei University, Xiamen, 361021, China

2 Nutritional Science and Epidemiology Group, School of Food Science and Nutrition, University of Leeds, Leeds, UK

3 Section of Natural and Applied Sciences, School of Psychology and Life Sciences, Canterbury Christ Church University, Canterbury, UK

Abstract: The adsorption of aflatoxin B_1 (AFB_1) to natural fiber materials prepared from corn by-products was investigated in this study. The results showed that corn cob powder (CCP) dose, particle size, time (0.25 to 24 h), temperature (4, 20, 37, 50 and 100°C) and pH (2 to 8), had significant effects on adsorption. The maximum adsorption (98%) was with particles 500-355 µm in size at 20°C for 8 h, at the dose of 50 $mg \cdot mL^{-1}$. The adsorption fitted pseudo-second-order model and Langmuir isotherm well. Besides, CCP had a higher adsorption capacity to AFB_1 than any single cell wall components of corn, which indicated that capillary effect happened in cell wall might be the main reason for adsorption. The results also suggested that CCP could reduce AFB_1 content from both liquid and solid food matrixes. Briefly, CCP displayed promising properties that could be developed in nature-based practical applications for food aflatoxin decontamination.

Key words: Aflatoxin B_1 Corn cob Adsorption By-products *Zea Mays*

1. Introduction

Aflatoxin B_1 (AFB_1) is a toxic metabolite by *Aspergillus* sp. that accumulates in many foods and feeds, especially in cereal and cereal-based food. These fungi grow in a wide range of geographical areas characterized by warm and humid conditions. The majority of countries set up AFB_1 maximum limit regulations for common grains given its serious toxic effect on human health. Strategies have been employed to prevent fungal growth and to remove the toxin from food. The strategies, include irradiation, treatment with neutral electrolyzed oxidizing water, microbial inhibition and degradation, and adsorption to synthetic and biological materials (Liu,

Abbreviation: AFB_1, aflatoxin B_1; CBP, corn bran powder; CCP, corn cob powder; EDTA, Ethylene Diamine Tetraacetic Acid; FB_1, fumonisin B_1; HPLC, high performance liquid chromatography; OTA, ochratoxin A; V_P, pore volume; S_{BET}, larger surface area; ZEN, zearalenone.

* Corresponding author. Email addresses: y.liu@jmu.edu.cn (Y. Liu)

† Corresponding author. Email addresses: c.orfila@leeds.ac.uk (C. Orfila)

Galani Yamdeu, Gong, & Orfila, 2020). Whilst some approaches can be simple, efficient, and eco-friendly, they may have issues such as loss of nutrients and sensory properties, the needs for specific equipment, or the introduction of inedible adsorbents to the system. Therefore, there is a need to investigate mycotoxin prevention of decontamination using materials that are food-grade/safe, sustainable, and widely sourced. For example, our previous study showed that the growth of *A. flavus* was inhibited by polyphenols extracted from citrus peel by-products (Liu, Benohoud, Galani Yamdeu, Gong, & Orfila, 2021).

In recent years, agricultural by-products have shown good capacity to adsorb various mycotoxins in buffer solutions (Table. S1). Greco, D'Ascanio, Santovito, Logrieco, and Avantaggiato (2019), used a mixed solution containing 1 $\mu g \cdot mL^{-1}$ of each AFB_1, zearalenone (ZEN), ochratoxin A (OTA) and fumonisin B_1 (FB_1), and found that pomegranate peel (55%), plantain peel (67%), almond hull (87%), carobs (100%) and grape pomaces (94%) all had strong adsorption to AFB_1, followed by ZEN; while pomegranate seed (86%), lemon residues (50% to 74%) and orange residues (51% to 61%) showed stronger adsorption to ZEN compared to the other three mycotoxins.

Corn or maize (*Zea mays*) is one of the most widely planted crops in the world. In 2019, the production of corn worldwide was about 1.15 billion tons. The major production regions are the Americas (49.20%), Asia (32.10%), Europe (11.60%) and Africa (7.10%) (FAOSTATS, 2021). As important by-products, about 18 kg of corn cob and 6 to 7 kg of corn bran can be generated for every 100 kg of corn grain (Choi, Nam, Yun, Kim, & Kim, 2022; Rose, Inglett, & Liu, 2010). These abundant corn by-products have been used as a feedstock for animal feed, production of biofuels, construction materials, absorbents for chemical waste, petrochemical industry and fermentation substrates (Choi et al., 2022; Rose et al., 2010).

The adsorption of various chemicals to carbonized or modified corn cob has been previously investigated. Corn cob (1.2 $mg \cdot mL^{-1}$) carbonized with H_2SO_4 was found to adsorb nearly 100% methylene blue in 1 h (Jawad, Mohammed, Mastuli, & Abdullah, 2018). Similarly, H_3PO_4-modified corn cob (after crude polysaccharide extraction) adsorbed up to 97.5% of malachite green at the dose of 5 $\mu g \cdot mL^{-1}$ (Hu et al., 2018). Biochar produced by pyrolysis of corn cob at 350°C and 450°C removed 8 to 73% of Pb^{2+} ions with different concentrations (0.25 to 3 $mg \cdot mL^{-1}$) of adsorbent doses (Assirey & Altamimi, 2021).

The hypothesis behind the adsorption ability of fiber-rich agricultural by-products is associated with their abundant functional groups of plant polysaccharides and lignin (e.g. hydroxyl, carbonyl, carboxylic/sulfhydryl carboxylic, phenolic, esters). These groups are suggested to be the active sites for adsorption (Rasheed et al., 2020). The cell wall of corn cob is primarily made of cellulose, cross-linked with hemicelluloses and lignin (Fig. S1). The proportion of these polysaccharides, as well as the composition of hemicelluloses, varies greatly between different corn varieties (Fig. S2). On average, cellulose, lignin (Fig. S1c) and hemicelluloses account for up to 42%, 35% and 46% respectively. Among the hemicelluloses, xylan is found to take up 26% to 33% of total cell wall dry weight, and is the most abound hemicellulose in the cob cell wall. When xylan units have arabinose as side groups (2.4% to 3.6% in corn cob), the polysaccharides are identified as arabinoxylan (Serra, Weng, Coelhoso, Alves, & Brazinha, 2020). These polysaccharides and lignin

contain abundant hydroxyls, esters, pyran rings, *etc*., which might be the functional groups involved in aflatoxin adsorption.

Adsorption technology is an important approach to remove small molecule hazardous materials from matrixes. For instance, clays have been shown to be effective adsorbents of AFB_1 and are used as technological additives to animal feed (Jaynes, Zartman, & Hudnall, 2007). Recently, biosorption has become an attractive option over other technologies due to showing high efficiency and excellent safety, as well as being environmentally friendly. Adsorption to microorganisms has been shown to be a promising technology (Table S2). For instance, adsorption of AFB_1 to yeast-based products could offer alternatives to clays and other additives (Campagnollo et al., 2020). Furthermore, adsorption of AFB_1 to the surface of lactic acid bacteria has been proposed to be through hydrophobic interactions, enhanced by sonication of the bacteria (Abedi, Mousavifard, & Bagher Hashemi, 2022). However, it can be difficult to compare between studies due to variation in culture and adsorption methodologies. Studies have demonstrated that the biomass from different agriculture by-products could adsorb hazardous materials, however, there is little data about the detoxification of AFB_1 by adsorption to non-charred corn by-products. Furthermore, few studies explore the mechanism of adsorption. Therefore, the present work was conducted to investigate the feasibility of using natural and simple prepared corn by-products as adsorbents to reduce AFB_1 content from aqueous solutions. The adsorption mechanism was characterised through adsorption model fitting and exploration of the adsorption of individual cell wall components. We discuss the potential of corn by-products as effective biosorbents of AFB_1, including their advantages and disadvantages compared to existing technologies. The present work also demonstrated the application of corn cob powder to detoxify AFB_1 in a number of food matrixes (grains and milk drinks), and the results suggested a new approach on AFB_1 reduction from liquid and solid foods before consumption.

2. Materials and methods

2.1 Materials

All chemicals and solvents (acetonitrile, methanol, ethanol) used were analytical grade. Cellulose (Cotton linters, microcrystalline, 9004-34-6) was purchased from Sigma (UK). Xylan (Beechwood, >95%, xylose/glucuronic Acid=80.8/11.4, 9014-63-5) and arabinoxylan (Rye, high viscosity, ~90%, arabinose/xylose=38/62, 9040-27-1) were purchased from Megazyme (Australia). Lignin (HY-111830) was from MedChem Express (UK). Cow's milk (Tesco whole milk, 3.7% fat), oat beverage (1.5% fat, 6.8% total carbohydrate, 1.4% dietary fiber, 0.3% protein), milled rice and pearl barley grain were purchased from local supermarket (Morrisons, UK). The fresh corn was purchased from local market (UK) in 2019. Commercial corn bran powder was obtained from local company (Dove's Farm, UK).

AFB_1 stock solution for adsorption experiments and quantitative analysis was prepared by dissolving 10 mg of AFB_1 (≥98%, Sigma, CAS 1162-65-8) in 1 mL of dimethyl sulfoxide (DMSO, Fluorochem, UK), and then diluted to 5 mL with acetonitrile to give a stock solution with the concentration of 2 $mg \cdot mL^{-1}$, stored at -20°C.

2.2 Preparation of corn by-product powder

The corn grains were manually removed from fresh corn cobs and the empty cobs were used as the first by-product material. Then the internal content of each grain was squeezed out with a pestle and the remaining bran was used for the other by-product material. Later, 500 g of corn by-products (corn bran or corn cob) were wet-milled (Breville, Australia) with 1 L of cold extraction buffer (50 mM Tris and 100 mM Ethylene Diamine Tetraacetic Acid (EDTA) containing 2.63 mM sodium metabisulphite) for 5 min at 4°C. Next, the blended sample was filtered through four layers of cheesecloth. The residue fractions were washed with water three times and then with acetone three times. After freeze drying, the dried corn by-product powder was sieved through test sieves (Endecotts, UK) to divide the powder into 5 fractions: >750, 700-500, 500-355, 355-250 and <250 µm. The powders were named as prepared corn cob powder (CCP) and prepared corn bran powder (CBP) respectively. Similarly, commercial CBP was dry milled for 5 min, and then was sieved as described above.

While corn is also one of the crops most susceptible to fungal and AFB_1 contamination, the contamination tends to concentrate on surface kernels, and not reach the cob. However, contamination of cob is always a possibility, therefore researchers should check the AFB_1 levels in CCP before starting their experiments.

2.3 Batch adsorption experiments with corn by-products

AFB_1 solutions for all adsorption experiments were prepared by diluting the stock solution (2 $mg \cdot mL^{-1}$) with milli-Q water to the concentration of 200 $ng \cdot mL^{-1}$. The effects of different conditions (powder particle sizes, CCP doses, incubation temperatures, incubation times, pH) were assayed. Activated charcoal (20-60 mesh) with AFB_1 solution (10 $mg \cdot mL^{-1}$) was used as positive control (Jaynes et al., 2007). The mixture was placed on a 100 rpm of shaking water bath at 20°C for 1 h. The 200 $ng \cdot mL^{-1}$ of AFB_1 solutions without adsorbents was used as negative control. After incubation, the suspended adsorbents were removed by centrifugation at 12000 rpm for 10 min. The supernatants were collected for AFB_1 determination by high-performance liquid chromatography (HPLC).

The efficiency (%) of AFB_1 adsorption to adsorbents was calculated as Eq.1:

$$\%\ \text{Adsorption} = \left(\frac{C_0 - C_t}{C_0}\right) \times 100 \quad (1)$$

Where, C_t is the concentration of AFB_1 in the solution after the adsorption process in $ng \cdot mL^{-1}$; and C_0 is the initial concentration of AFB_1 in $ng \cdot mL^{-1}$.

2.4 Model studies of AFB_1 adsorption

2.4.1 Adsorption kinetic study

Kinetic models of adsorption help to describe the process of adsorption (Rasheed et al., 2020). The experiment was carried out by adding 3 mg of CCP to 300 µL of AFB_1 solution at a concentration of 60 µg·mL^{-1}. The mixture was placed on the shaking water bath (100 rpm) at 20°C. After centrifugation, the supernatant containing residual AFB_1 was measured from 5 min to 24 h with HPLC. The equilibrium was achieved when there was no noticeable change in % adsorption after this time point.

The adsorption capacity of CCP for AFB_1 was calculated as Eq.2 (Ji & Xie, 2021):

$$q_e = \frac{(C_0 - C_e)V}{m} \quad (2)$$

Where q_e is the adsorption amount of AFB_1 at equilibrium condition in µg·mg^{-1}; C_0 is the initial concentration of AFB_1 in µg·mL^{-1}; C_e is the equilibrium concentration of AFB_1 after adsorption process in µg·mL^{-1}; V is the volume of AFB_1 solution in mL; m is the weight of CCP in mg.

The experimental data from present study could be fitted to two classic kinetic models, pseudo-first-order Eq.3 and pseudo-second-order Eq.4:

$$ln\frac{q_e - q_t}{q_e} = -k_1 t \quad (3)$$

$$\frac{t}{q_t} = \frac{1}{k_2 q_e^2} + \frac{t}{q_e} \quad (4)$$

Where t is the adsorption time in min; q_t is the adsorption amount of AFB_1 at time point t in µg·mg^{-1}; k_1 is the rate constant of pseudo-first-order in 1/min; k_2 is the rate constant of pseudo-second-order in mg·(µg·min)$^{-1}$. The linearized plots for pseudo-first-order and pseudo-second-order model were estimated using the slope and intercept of $\ln(q_e\text{-}q_t)$ vs. t and (t/q_t) vs. t respectively.

The root mean square error (RMSE) of the calculated data related to the experimental data could be estimated as Eq.5 (Abedi, Pourmohammadi, Mousavifard, & Sayadi, 2022):

$$RMSE = \sqrt{\frac{(experimental\ data - \text{calculated data})^2}{n-p}} \quad (5)$$

Where n is the number of experimental data; p is the number of variables.

Moreover, the experimental data could be calculated as the intraparticle diffusion model Eq.6 (Ma, Cai, Mao, Yu, & Li, 2021):

$$q_t = k_{id} t^{0.5} + c \quad (6)$$

Where k_{id} is the rate constant of intraparticle diffusion model in µg·(mg·min$^{-0.5}$)$^{-1}$; C is to reflect the thickness of the boundary layer in µg·mg^{-1}. The plot for the intraparticle diffusion model was estimated using the slope and intercept of q_t vs. t. The intercept of the plot reflects the thickness of the boundary layer.

2.4.2 Adsorption isotherm models

Adsorption isotherm models are applied to describe the maximum adsorption capability of AFB_1 adsorbed on CCP and molecules under different initial concentrations at a constant temperature (Rasheed et al., 2020). The experiment was performed at 20°C by adding 3 mg of CCP to 300 µL of AFB_1 solution at various initial concentrations from 0.1 to 90 µg·mL^{-1}. The mixture was placed on the shaking water bath (100 rpm) immediately until adsorption equilibrium.

The adsorption isotherms data could be conducted using Langmuir Eq.7 and Freundlich Eq.8 models (Avantaggiato, Greco, Damascelli, Solfrizzo, & Visconti, 2013):

The Langmuir model is presented as $q_e = \frac{q_m k_L C_e}{1+k_L C_e}$ (7)

Where k_L is the Langmuir constant in mL·µg^{-1}; q_m is the maximum adsorption capacity in µg·mg^{-1}. The parameters for the Langmuir model were estimated by plotting C_e/q_e vs. C_e.

The Freundlich model is presented as $q_e = k_F C_e^{\frac{1}{n}}$ (8)

Where k_F is the Freundlich constant in mL·µg^{-1}; 1/n is the degree of heterogeneity of adsorbent surface. The parameters for the Freundlich model were estimated by plotting $\ln q_e$ vs. $\ln C_e$

2.4.3 Adsorption thermodynamic study

Adsorption thermodynamics study can also provide theoretical evidence of the feasibility and spontaneity of the adsorption reaction (Rasheed et al., 2020). This experiment was carried out by adding 3 mg of CCP to 300 µL of AFB_1 solution at concentration of 60 µg·mL^{-1}. The mixture was placed on the shaking water bath (100 rpm) immediately at various temperature (20 to 50°C) until adsorption equilibrium.

The thermodynamic constants were calculated by the van't Hoff Eq.9-12. The constants were the Gibbs free energy (ΔG^0), standard entropy change (ΔS^0) and standard enthalpy change (ΔH^0) (Ji & Xie, 2021).

$$K_T = \frac{q_e}{C_e} \quad (9)$$

$$\Delta G^0 = -RT ln K_T \quad (10)$$

$$\Delta G^0 = \Delta H^0 - T\Delta S^0 \quad (11)$$

$$ln K_T = \frac{\Delta S^0}{R} - \frac{\Delta H^0}{RT} \quad (12)$$

Where K_T is the equilibrium constant in mL·mg^{-1}; ΔG^0 is the Gibbs free energy of adsorption in kJ·mol^{-1}; R is the general gas constant 8.314 J·(mol·K)$^{-1}$; T is the adsorption absolute temperature in K; ΔH^0 is the enthalpy change in kJ·mol^{-1}; ΔS^0 is the entropy change in J·(mol·K)$^{-1}$. The plot for

the van't Hoff equations was estimated using the slope and intercept of $\ln K_T$ vs. 1/T, and the slope and intercept approximately equalled to $-\Delta H^0/R$ and $\Delta S^0/R$ respectively.

2.5 Adsorption stability of CCP-AFB_1 complex after several washes

According to Assaf, El Khoury, Atoui, Louka, and Chokr (2018), following the adsorption experiment with CCP (500-355 µm) as previously described, the adsorption stability was focused on the CCP-AFB_1 complex. Twenty mg of CCP was added in 2 mL of 200 ng·mL^{-1} AFB_1 solution and then incubated at 20°C for 1 h. Next, the mixture was poured into a filtration column (15 mL, TELOS, US) for washing steps (Fig. S3). The complex was washed with 2 mL of water or ethanol 5 times each, and every wash took 10 min. The washed AFB_1 content was quantified by HPLC.

2.6 Adsorption experiment with cell wall components

Commercial cellulose, lignin, arabinoxylan and xylan were used in the adsorption experiment following the same binding experiments as described for CCP and CBP. 10 mg of each standard were incubated with 1 mL of 200 ng·mL^{-1} AFB_1 solution at 20°C for 1 h. Tube was then centrifuged at 12000 rpm for 10 min. The supernatant was collected for AFB_1 content detection by HPLC, and the % adsorption was calculated as described before.

2.7 Application of CCP for AFB_1 removal from food matrixes

To evaluate the potential practicability of the CCP, two types of food matrixes were used (Fig. S4). For liquid food matrixes (Fig. S4a), 2 mL of milk or oat beverage was firstly spiked with 400 ng of AFB_1, and then 20 mg of prepared CCP (500-355 µm) was added into the liquid. After 1 h incubation at 20°C, the suspended CCP was removed by centrifugation as described above. In order to extract AFB_1 from matrixes, 1 mL of supernatant was collected and diluted with 1 mL of water, and the mixture was loaded into a pre-conditioned Oasis Max column (Waters, UK). The column was washed with 5 mL of distilled water, and then AFB_1 was eluted from the column with 2 mL of methanol. Finally, the AFB_1 elution solution was diluted to 4 mL with 10% methanol. The milk or oat beverage containing AFB_1 (200 ng·mL^{-1}) without adsorbents was used as negative control. The % removal was calculated by comparison with the negative control.

For solid food matrixes (Fig. S4b), rice or barley spiked with AFB_1 were used to simulate grains contaminated by the toxin, and investigate the removal of AFB_1 while washing the grain with added CCP. Five grams of milled rice or barley spiked with 2000 ng of AFB_1 were soaked in 10 mL of water containing 100 mg CCP (500-355 µm) for 1 h at 20°C. The grains were then separated from the soaking solution, and washed with 10 mL of water to remove the CCP remaining on the grains. Finally, 10 mL of neat acetonitrile was applied to extract AFB_1 on the grain by soaking for 5 min. The acetonitrile extraction solution was dried by Genevac (Fisher Scientific, UK), and then diluted with 10mL of 50% methanol which was analyzed by the method specified in 2.8. The rice or barley spiked with AFB_1 and washed without adsorbents was used as negative control. The % removal was calculated by comparison with the negative control.

2.8 AFB_1 quantification

AFB_1 quantification was carried out according to the report by Ma et al. (2021) with some modifications. The measurement was performed on a Shimadzu (Japan) HPLC system coupled with a fluorescence detector (RF-20A xs). The AFB_1 samples (50 µL) were injected into a Phenomenex Luna C18 column (5 µm particle size, 150×4.6 mm) operated at 40°C. The mobile phase was composed of HPLC grade water: acetonitrile: methanol (70:15:15/vol:vol:vol). An isocratic gradient was run and its flow rate was 1 $mL \cdot min^{-1}$. Fluorescence detection was used with excitation and emission wavelengths of 360 and 440 nm, respectively. The retention time for AFB_1 was 23.1 min. A calibration curve was established using different concentrations of AFB_1 standard ranging from 3.125 to 200 $ng \cdot mL^{-1}$ (R^2=0.9997). The limit of detection was 0.1 $ng \cdot mL^{-1}$. The recovery (%) of AFB_1 by Oasis Max column from aqueous solution, milk and oat beverage was 105.32%, 118.05% and 73.94% respectively, and this value was 92.16% and 83.26% from rice and barley respectively.

2.9 Statistical analysis

Data were analyzed by one-way ANOVA and Tukey's multiple range tests using GraphPad 7. Model fitting was performed by Origin2018. All results are shown as the mean value ± standard deviation of triplicate experiments ($P< 0.05$).

3. Results and discussion

3.1 Factors affecting AFB_1 adsorption by corn by-products

The effect of several factors, including material type, powder particles sizes, dosage, incubation time, temperature and pH, on the adsorption of AFB_1 to corn by-products in aqueous solution was evaluated.

To screen the best corn by-product for AFB_1 adsorption, batch adsorption experiments were performed with prepared CBP, prepared CCP, and commercial CBP under different conditions. As shown in Fig. 1a, apart from particle sizes >750 µm, the adsorption of prepared CCP (79.54% to 90.02%) was consistently higher than that of prepared CBP (64.52% to 66.13%) and commercial CBP (39.20% to 47.33%). Corn bran is characterized by a porous pericarp layer with a thickness of 100 to 250 µm (Roye et al., 2019). Nevertheless, corn cob generally contains an inner pith layer of a closed cellular structure type, a middle wood ring layer of cross-interconnected sponge-like vascular pores, and the outer glume layer of squeezed bran (Fig. S5) (Zou, Fu, Chen, & Ren, 2021). Thus, the CCP containing three types of structure might explain a higher adsorption ability than a single layer of CBP.

From the perspective of particle size (Fig. 1a), the adsorption of all three adsorbents was significantly affected by particle size (p<0.005). For CCP, compared to the smallest size (<250 µm), when the size was larger than 500 µm, the adsorption significantly decreased to 56.12%

(p<0.005), whereas the powder with size smaller than 500 µm showed no significant effect on % adsorption (86.49% to 90.03%) (p>0.05). In another study, a similar trend could be found in mycotoxin adsorption with grape pomace particles. This might be because larger particles have fewer accessibility to adsorption sites for mycotoxins, compared to smaller ones (Avantaggiato et al., 2013). As the CCP showed the best effect on AFB_1 adsorption, it was selected as the adsorbent for further studies.

Batch adsorption experiments showed a strong significant effect of CCP doses on AFB_1 adsorption (p<0.0001) (Fig. 1b). The results indicated that the adsorption increased linearly from 23.16% to 97.99% by increasing the adsorbent dose from 1 to 50 $mg \cdot mL^{-1}$. This indicated that higher doses of CCP provided more adsorption sites resulting in larger % adsorption. Similar results have been reported in other AFB_1 adsorption materials. For example, the adsorption capability of blueberry pomace increased from 16% to 79% by increasing the dosage from 0.5 to 3.0 $mg \cdot mL^{-1}$ (Rasheed et al., 2020). The toxin removal of a synthetic magnetic adsorbent, Fe_3O_4@ATP, significantly improved (54% to 87%) with an increase in the dosage from 0.5 to 3 $mg \cdot g^{-1}$, and then the removal ability approached constant levels from 0.3 to 1.0 $mg \cdot g^{-1}$ (Ji & Xie, 2021). Somewhat differently, modified organo-rectorites (ORts) as AFB_1 adsorbent showed an increasing adsorption (65% to 89%) with the dosage ranging from 0.5 to 2.0 CEC (cation exchange capacity), while the % adsorption decreased to 82% at the dosage of 2.5 CEC. This was because large dosage (2.5 CEC) of modifier molecules could aggregate together and congregate on the Orts surface, which reduced the proportion of active ingredients in the adsorbent (Sun, Song, Wang, Wang, & Zheng, 2018).

The dependence of Incubation times on % AFB_1 adsorption was investigated and found to be a significant factor (p<0.0001) (Fig. 1c). Over 80% of the total adsorption occurred in the first 15 min. With the increase in incubation time, the adsorption efficiency increased gradually up to 93.46%, and this maximum adsorption was reached at 8 h. Then the adsorption efficiency remained stable in the next 16 h, suggesting a state of equilibrium had been reached. Guo, Yue, Hatab, and Yuan (2012) reported that the adsorption of commercial yeast powder and patulin reached to highest point (about 100%) at 30 h, while that of lab-prepared yeast powder was 6 h later (about 100%). Palade, Dore, Marin, Rotar, and Taranu (2020) found AFB_1 adsorption occurred rapidly (<5 min) by the food or agricultural by-products (carrot, celery, granny apple, red potato, white potato, and sea buckthorn) accompanied by the increase until 200 min; similarly, the adsorption of ZEN could be seen at less than 5 min and its maximum binding was observed at 90 min. Avantaggiato et al. (2013) demonstrated that around half of mycotoxins (AFB_1, ZEN, OTA, and FB_1) in a mixed solution was adsorbed by grape pomace in less than 3 min, and the maximum adsorption occurred in 15 min. Therefore, it can be seen that the fixation between mycotoxins and adsorbents happens rapidly, and a predominant amount of total mycotoxins would be adsorbed in the early stage. Once the adsorption was stable, the free adsorbates (toxins) in the solution would not significantly decrease.

The AFB_1 adsorption experiments were subsequently conducted at 5 different temperatures, 4°C, 20°C, biological temperature (37°C), warm temperature (50°C), and boiling temperature (100°C) for 1 h (p<0.0001). Fig. 3d shows that, apart from 100°C (decreased to 71.74%) (p<0.0001), the

adsorption of AFB_1 over cob powder was independent of temperature, with binding of 84.18% at 4°C, 84.47% at 20°C, 84.96% at 37°C, and 86.97% at 50°C (p>0.05). Therefore, CCP could be used in a wide range of temperatures used in food processing for AFB_1 adsorption/removal. The effect of temperatures on AFB_1 adsorption was also investigated by previous studies. The by-products of grape seed (approximately 45%) and sea buckthorn (approximately 35%) did not significantly change the AFB_1 adsorption ability at 25°C, 37°C and 40°C (Palade et al., 2020). However, temperature significantly affected the adsorption behavior of two novel materials. Fe_3O_4@ATP adsorbed 83% of AFB_1 from peanut oils at 40°C, and the % adsorption increased by 5.85% with increasing temperature to 60°C, while fell back to 82.02% when the temperature continuously raised to 110°C (Ji & Xie, 2021). Besides, the AFB_1 adsorption to mesoporous silica prepared from rice husk kept stable (around 95%) in an oil matrix between 10°C to 20°C, but decreased sharply to 75% when the temperature increased to 30°C (Li et al., 2020). These studies indicated that the effect of temperature on adsorption varies depending on the materials.

To evaluate the adsorption of AFB_1 to CCP as a function of pH, batch adsorption tests were performed with pH ranging from 2 to 8 (Fig. 1e). The result revealed that the pH of adsorption solutions had had a small but significant effect on the adsorption (83.81% to 87.18%) of AFB_1 to CCP (p<0.05). However, compared to pH 7, most of the pH conditions did not significantly affect the adsorption (p>0.05), apart from pH 5. pH is a key factor impacting the surface charge of adsorbents and the ionization level of toxins (Zahoor & Ali Khan, 2014). In general, the adsorption ability of toxins has been shown to be greatly affected by pH, such as malachite green adsorbed by acidified corn cob (Hu et al., 2018), ZEN, OTA, and FB_1 adsorbed by grape pomace (Avantaggiato et al., 2013), and methylene blue adsorbed by carbonized corn cob (Jawad et al., 2018). However, there is no ionization on the AFB_1 molecule under different pH conditions (Sun et al., 2018). Therefore, not only the adsorption of CCP on AFB_1 was not strongly affected by pH at a range from 2 to 8 in the present study, but also in the adsorption to iron oxide carbon nanocomposites (prepared from bagasse) (Zahoor & Ali Khan, 2014), blueberry pomace (Rasheed et al., 2020) and grape pomace (Avantaggiato et al., 2013). AFB_1 (Fig. 1f) is a non-ionizable molecule and does not have hydrophilic groups, such as -COOH and -OH (Ma et al., 2021). As the components of natural cob do not carry strong charges, the adsorption of AFB_1 on CCP may not be strongly affected by pH (Abbas et al., 2018). This result indicated that the CCP can be considered as an AFB_1 adsorbent in liquid foods under most pH conditions, and that the binding is likely through interactions other than electrostatic.

The levels of adsorption of AFB_1 to CCP are of a similar order of magnitude to the adsorption to lactic acid bacteria (Abedi, Pourmohammadi, et al., 2022) and yeasts (Campagnollo et al., 2020). Interestingly, the adsorption to lactic acid bacteria cell wall was enhanced by sonication which is proposed by the authors to increase surface hydrophobicity through structural effects on cell wall proteins (Abedi, Mousavifard, et al., 2022). It would be interesting to investigate the effect of such physical treatment on CCP in future research.

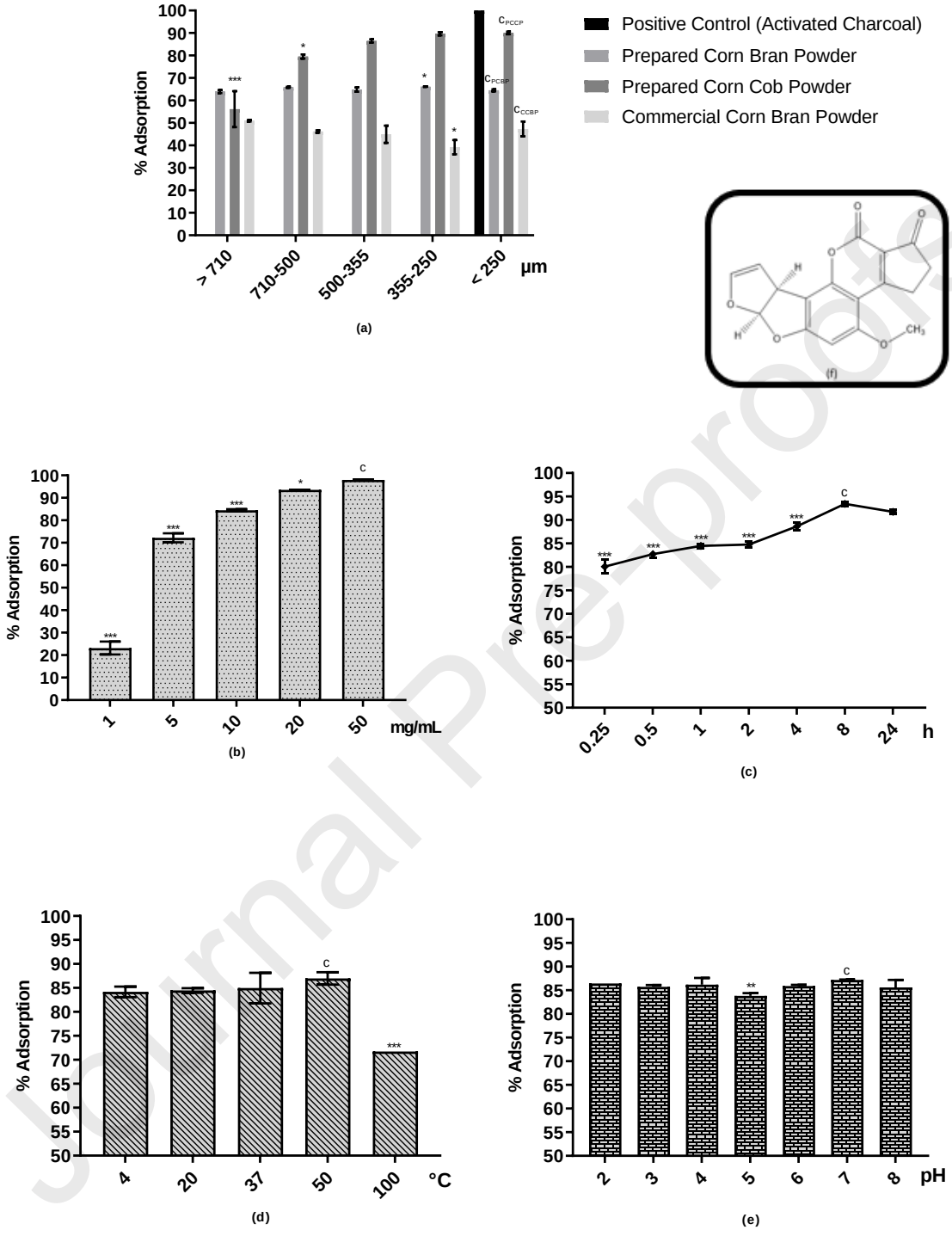

Fig. 1 The % Adsorption of CBP and CCP to AFB_1 affected by particle sizes (a), CCP doses (b), incubation times (c), incubation temperatures (d) and pH (e), and chemical structure (f) of AFB_1. * represents significant differences between different groups to the group (C) showing the highest AFB_1 % adsorption. ***, $p \leqslant 0.0001$; **, $p \leqslant 0.001$; *, $p \leqslant 0.05$. Results are means of three replicates.

3.2 Model studies of AFB_1 adsorption

3.2.1 Adsorption kinetic study

In kinetic study, the adsorption capacity of CCP to AFB_1 raised rapidly within 5 h (Fig. S6a), presumably caused by the strong capillary force formed by microporous and mesoporous material in the cob powder (Ma et al., 2021). Then the equilibrium was achieved in 8 h. To analyse the controlling mechanism of the adsorption process, two classic models (pseudo-first-order and pseudo-second-order) were applied. The fit of the pseudo-first-order (eq. 3) to AFB_1 adsorption data is shown in Fig. S6b and the pseudo-second-order (eq. 4) in Fig. 3Sc. The kinetic parameters are listed in Table. 2. According to the result, the pseudo-second-order model (R^2=0.9979) better fitted the data than the pseudo-first-order model (R^2=0.7727). Meanwhile, the RMSE values in the pseudo-second-order model (0.0188) was much lower than the pseudo-first-order model (0.4271). This suggests the AFB_1 adsorption process involves chemisorption (Ji & Xie, 2021; Ma et al., 2021; Pourmohammadi, Sayadi, Abedi, & Mousavifard, 2022).

In general, the near-adsorbent adsorption process involves three steps, which are 1) boundary layer diffusion which is when adsorbate diffusion occurs across the liquid film surrounding the adsorbent; then 2) intraparticle diffusion which is further diffusion within internal pores of adsorbent; finally 3) adsorption of adsorbate on the surface of adsorbent (Ma et al., 2021). Moreover, the boundary layer and/or intraparticle diffusion is generally the controlling step, and the last step is relatively fast in the majority of adsorption systems (Ma et al., 2021). Therefore, the intraparticle diffusion model (eq. 6) is usually conducted to fit the experimental results for the explanation of the diffusion mechanism. The intraparticle diffusion plot (Fig. 3Sd) displayed two-linearity in the adsorption of AFB_1 on CCP, which indicated that the adsorption process involved the diffusion of AFB_1 from solution to the boundary layer of cob powder and the intraparticle diffusion into the porous structure of cob powder at low concentration of AFB_1 to final equilibrium (Cai, Liu, Tian, Yang, & Luo, 2019; Ma et al., 2021). The plot did not pass through the origin, so the boundary layer diffusion and intraparticle diffusion controlled the rate-controlling step (Ma et al., 2021). It is reported that the meso- and microporous morphology presents an easy accessibility of adsorbates into the internal structure of the adsorbents, while the micropores are narrow for adsorbates to access the adsorbents so that limit the inner diffusion rate of adsorption (Ma et al., 2021). Therefore, the cob powder might have a large portion of meso- and macropores, while having a small portion of micropores (Ma et al., 2021). In addition, the intercept of the intraparticle diffusion plot (C) suggested the thickness of the boundary layer (Table. 2), reflecting the contribution of the boundary layer in the adsorbate adsorption rate (Ma et al., 2021).

Table. 2 Kinetic parameters of pseudo-first-order, pseudo-second-order and intraparticle diffusion for the adsorption of AFB_1 on CCP (20°C)

	$q_{e,exp}$ (μg·mg^{-1})	$q_{e,cal}$ (μg·mg^{-1})	R^2	RMSE

		k_1 (1/h)			
Pseudo-first-order					
	2.9910	-0.0071	1.5746	0.7727	0.4271
		k_2 (mg·(μg·h)$^{-1}$)			
Pseudo-second-order					
		0.37075	3.0533	0.9979	0.0188
		k_{id} (μg·(mg·h$^{0.5}$)$^{-1}$)	C		
Intraparticle diffusion	-				
		0.5852	0.7247	0.8386	-

$q_{e,exp}$, the experimental adsorption capacity; $q_{e,cal}$, the calculated adsorption capacity.

3.2.2 Adsorption isotherm models

Two non-linear isotherm models were used to investigate the adsorption characteristic: Langmuir (eq. 7) and Freundlich (eq. 8) isotherm models. The Langmuir model is one of the most classic models describing an ideal adsorption with the characteristics of a monolayer, no interaction between adsorbates, and uniqueness of all adsorption sites on the adsorbent surface (Ma et al., 2021). Whereas, the Freundlich model is the earliest isotherm used to describe the adsorption performance on a heterogeneous surface, not restricted to the formation of monolayer (Avantaggiato et al., 2013). The linear regression fitting figures of the two models can be found in Fig. S7a and b, and the parameters are listed in Table. 3. From the results of the present study, the Langmuir isotherm demonstrated a better fit with the experimental data (R^2=0.9986) than the Freundlich model (R^2=0.9344). This suggests that the isothermal adsorption by CCP could be better described by the AFB_1 adsorption on the homogeneous CCP surface and no further adsorption occurs once AFB_1 molecules are adsorbed at specific sites on cob powder (Sun et al., 2018). According to the Langmuir model, the maximum adsorption capability of CCP was calculated to be 3.1268 μg·mg^{-1}. This AFB_1 adsorption capability was far higher than banana peel (0.0084 μg·mg^{-1}) (Shar et al., 2016), but similar to grape pomace (2.8600 μg·mg^{-1}) (Avantaggiato et al., 2013) and blueberry pomace (3.2290 μg·mg^{-1}) (Rasheed et al., 2020). Moreover, k_L is a constant related to the energy and affinity of CCP, which indicates that the adsorption was favourable when k_L was above 0 (Ma et al., 2021).

Table. 3 Isotherm model parameters for the adsorption of AFB_1 on CCP (20°C)

			R^2
	q_m (μg·mg^{-1})	k_L (mL·μg^{-1})	
Langmuir model			
	3.1268	0.3109	0.9986
	1/n	k_F (mL·μg^{-1})	
Freundlich model			
	0.6325	0.4057	0.9344

3.2.3 Adsorption thermodynamics study

In the adsorption thermodynamics study, the van't Hoff plot and thermodynamics parameters (eq. 9-12) for the adsorption of AFB_1 on CCP were demonstrated in Fig. S8 and Table. 4 respectively. For this AFB_1 adsorption, the equilibrium constant K_T decreased with increasing temperature, which means the experimental and theoretical adsorption capacities declined with the increased temperature, as well as the absolute Gibbs free energy change (ΔG^0) rose with the increased temperature. This indicated that higher temperatures lowered the adsorption driving force (Ji & Xie, 2021). However, the positive ΔG^0 at all temperatures suggested the adsorption process occurred non-spontaneously at certain temperatures (Avantaggiato et al., 2013). Furthermore, the enthalpy change (ΔH^0) in this adsorption process was negative confirming the reaction was exothermic. The magnitude of value ΔH^0 can also describe the type of adsorption (either physical or chemical adsorption). Generally, physical adsorption is rapid and weak, and the interactions include hydrogen bonds, van der Waals, dipole-dipole, and induced dipole; while chemical adsorption is highly specific and slow, as well as the interaction exists electron transfer between molecules, e.g. covalent bonds (Avantaggiato et al., 2013; Karakaya, 2011). When ΔH^0 <20 kJ·mol^{-1}, the adsorption is considered as physisorption, whereas chemisorption is generally described as having ΔH^0 >20 kJ·mol^{-1} (Avantaggiato et al., 2013). In the adsorption of AFB_1 on CCP, the ΔH^0 was -19.1060 kJ·mol^{-1}, which suggested a physical adsorption. In the kinetic study, the proposed mechanism involved layer diffusion and the involvement of meso- and macro structures, though chemical adsorption could not be ruled out. Thus, both chemical and physical adsorption might exist in this process (Hu et al., 2018). In the solid-liquid system, a natural adsorption of the adsorbate onto the adsorption surface would lower the chaos of the system, which is represented by the entropy change (ΔS^0) below 0 (Hu et al., 2018). In the present work, the ΔS^0 was found to be -0.0824 kJ·(K·mol)$^{-1}$, illustrating the randomness of AFB_1 molecules on the CCP interface reduced with the increasing temperature (Rasheed et al., 2020). It is believed that this phenomenon corresponds to polar non-covalent interactions (Avantaggiato et al., 2013). In a

word, in terms of the thermodynamics parameters, the adsorption process of AFB_1 on CCP was an exothermic and chaos-reduced adsorption interaction.

Table. 4 Thermodynamics parameters for the adsorption of AFB_1 on CCP

Temperature (K)	K_T	$\ln K_T$	ΔG^0 (kJ·mol^{-1})	ΔH^0 (kJ·mol^{-1})	ΔS^0 (kJ·(K·mol)$^{-1}$)	R^2
293	0.1195	-2.1249	5.0460			
303	0.1069	-2.2363	5.8703			
				-19.1060	-0.0824	0.9589
313	0.0744	-2.5987	6.6946			
323	0.0598	-2.8163	7.5189			

3.3 Adsorption stability after successive washes in water or ethanol adsorbed with AFB_1

After 1 h incubation of CCP with AFB_1, the adsorption stability of the complex was assessed by quantifying AFB_1 in each washing liquid. As shown in Fig. S9, AFB_1 was released from the complex after washes by either water or ethanol. In the first two washes of water, 10.42% and 8.80% of total AFB_1 (200 ng·mL^{-1}) were washed off respectively, and around 6% to 7% of that was released in the rest of each successive washes. After five-time wash, around 46% of the total adsorbed AFB_1 (168.94 ng) was eluted. Conversely, ethanol removed 67.68% of total AFB_1 (200 ng) from the complex in the first wash, and AFB_1 was desorbed from 10.26% to 1.33% during the remaining four washes. Thus, nearly all the adsorbed AFB_1 was released from CCP. The reversibility indicated that these non-specific and weak adsorption non-covalent bonds formed between CCP and AFB_1 could be disrupted after successive washes (Abedi, Pourmohammadi, et al., 2022; Assaf et al., 2018; Karakaya, 2011). As AFB_1 is soluble in ethanol, while sparingly soluble in water, the adsorption was more unstable by the disruption of ethanol than water. Therefore, CCP as the adsorbent to remove AFB_1 in food matrixes should be replaced once the adsorption reaches equilibrium.

3.4 Proposed adsorption mechanism for aflatoxins on CCP

In this study, commercial cellulose, lignin, xylan and arabinoxylan were used to investigate potential molecular mechanisms of AFB_1 adsorption to CCP. As shown in Fig. 3, these isolated components all had various degrees of lower AFB_1 adsorption capability compared to CCP at the

same dose. There was little adsorption of AFB_1 to xylan, while cellulose and arabinoxylan showed low adsorption at 8.16% and 14.03% respectively. However, lignin displayed surprisingly high (63.43%) adsorption efficiency. On the one hand, corn cob gave strong signals in some hydrophilic characteristic peaks (e.g. -OH stretching of hydroxyl groups, -CO groups stretching in ether). These might establish hydrogen bonds with 'O atoms' of -C=O groups of AFB_1, which could provide strong dipole-dipole interaction in the adsorption (Rasheed et al., 2020). On the other hand, CCP also has hydrophobic groups (e.g. -CH, -C=C, aromatic subunits in lignin, and the ferulic acid of arabinoxylan) which might enable hydrophobic interactions with AFB_1 (Ojedokun & Bello, 2017). In a study of AFB_1 removal by metal-organic framework materials, with the carbonization temperature rising (uncarbonized, 400°C, 600°C and 800°C), the intensities of -OH peaks in the material gradually disappeared, suggesting an increasing hydrophobicity of the material surface. The sample carbonized at high temperatures (600°C and 800°C) displayed the highest AFB_1 removal capability (Ma et al., 2021). This suggested that the hydrophobic treatment of corn cob might improve the AFB_1 adsorption to some extent. The involvement of hydrophobic interactions in AFB_1 adsorption was also suggested by Abedi, Pourmohammadi, et al. (2022). In this study, AFB_1 was adsorbed by lactic acid bacteria, and it should be noted that the cell walls of these bacteria contain significant higher amounts of protein and that proteins have more potential of forming hydrophobic patches on surfaces compared to cellulosic or other carbohydrate material. The binding to corn cell wall proteins (e.g. extensins, arabinogalactan proteins) should be further investigated.

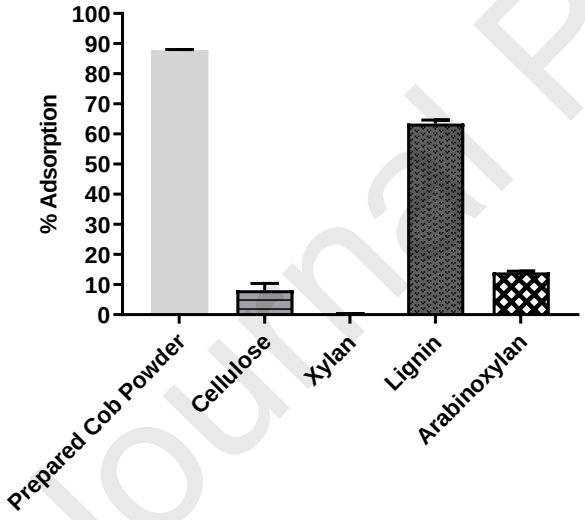

Fig. 3 % Adsorption of corn cob cell wall components (10 mg) to AFB_1 (200 $ng \cdot mL^{-1}$) for 1 h at 20 °C.

Based on the present work, however, even at the same amount, the % adsorption of any single cob component was far less than the natural cob powder. Considering that each component accounted for a portion of the total weight of corn cob, the role of individual components in

adsorption might be very limited. Therefore, the adsorption may not only depend on the interaction between AFB_1 with cell wall components, but also on a significant effect of cob cellular organizational structure on adsorption properties. In general, larger surface area (S_{BET}) and pore volume (V_P) causes a higher adsorption capacity on adsorbents, as they can provide more sorption sites and space. For natural corn cob, the S_{BET} and V_P was 93.46 $m^2 \cdot g^{-1}$ and 0.0577 $cm^3 \cdot g^{-1}$ respectively, and one nearly-planar AFB_1 molecule normally occupied 1.38 nm^2 surface area, so that the CCP could provide large amount of adsorption sites and space for AFB_1 adsorption (Chukwuemeka-Okorie, Ekemezie, Akpomie, & Olikagu, 2018; Ma et al., 2021). In addition, the adsorption also depends on the molecular size of adsorbates and the pore size of adsorbents. When the molecule size of adsorbates is larger than pore diameter, there is no adsorption process occurring because of the steric hindrance; when the molecule size approximately equal to pore diameter, the adsorbates can be strongly captured by the adsorbents and no easy desorption due to the superposition of potential energy fields in adjacent wall pores; while the molecule size of adsorbates smaller than pore diameter can take place capillary condensation easily in the pores of adsorbates to improve the adsorption capacity (Zhu, Shen, & Luo, 2020). For AFB_1 molecule, the micropores (<2.0 nm) of the adsorbents were found to impede the diffusion of AFB_1, while AFB_1 could be directly adsorbed with mesopores (2.0 to 50.0 nm) by the capillary effect (Galvano et al., 1996; Ma et al., 2021). The average pore sizes of CCP were estimated to be about 18 to 25 nm, and mesopores took up 27.40% of total pores in the raw cob (Chukwuemeka-Okorie et al., 2018; Ji, Lin, Chen, Dong, & Imran, 2015). Thus, it could be postulated that the capillary effect that happened in the mesopores might be the main reason for the adsorption of AFB_1 by CCP.

3.5 Application of CCP for AFB_1 removal from food matrixes

The extent of AFB_1 removal by CCP from food model matrixes is listed in Table. 5. The removal of AFB_1 by CCP in milk was 29.01% ($p<0.001$) lower than that in AFB_1 aqueous solution, and this value was lower (22.59%) in oat beverage. This could be because proteins or other macromolecules in these drinks could have interactions with AFB_1 or CCP, which might reduce the accessibility of the toxin to the adsorbent. There could be competitive adsorption between proteins and adsorbent; while the different types and contents of protein in milk and oat beverage could explain the discrepancy between the two beverages (Harshitha et al., 2022; Rafique et al., 2022).

In the process of contaminated grain washing, some of AFB_1 (35.55% for rice and 22.71% for barely) could be removed by prolonged soaking (1 h) in water, and a little would be removed by rapid rinsing later (5.11% for rice and 5.52% for barley). Thus, about 40% of AFB_1 from rice and 28% from barley was reduced by 'pre-washing'. Once the CCP was added during soaking, 72.47% of remaining AFB_1 on rice or 52.55% on barley was additionally removed compared to negative control group (Fig. 4). It can be observed that the surface of rice was densely packed with starch granules (Bonto, Tiozon, Sreenivasulu, & Camacho, 2021), while there was a loose and porous aleurone layer on the outside of the barley endosperm (Jääskeläinen, Holopainen-Mantila,

Tamminen, & Vuorinen, 2013). This difference in grain structure might be the main reason for the different removal effects of CCP on AFB_1. This approach of using CCP as a grain washing step may also be interesting in animal feeding, compared to adding adsorbents directly to the feed. For instance, the study by Jaynes et al. (2007) showed that various clays could adsorb AFB_1 in corn meal, but the risk of aflatoxicosis due to the likely desorption in the digestive tract could not be ignored.

In short, although CCP showed different behaviors of AFB_1 removal in various matrixes, it could still be a promising adsorbent for the removal of AFB_1 in foods. For instance, filter or padding produced from CCP could be applied in the detoxification of liquid foods or contaminated water, while the CCP can be also added to water directly when washing contaminated grains before consumption. However, it is also worth noting that concomitantly to AFB_1 removal, nutrient losses may occur due to the adsorption of nutrients by adsorbent; while the components in food matrixes might interact with AFB_1 that could decrease adsorption capability by CCP. This needs to be investigated in the future. Moreover, the further study should focus on the maximum adsorption in different food matrixes.

Table. 5 AFB_1 removal (%) by CCP in different food matrixes

Matrixes	% Removal [a]	Matrixes	% Removed by soaking only	% Removed by rinsing only	% Removal [a]
Aqueous solution	87.84±1.26				
Milk	58.83±2.75***	**Rice**	35.55±0.68	5.11±1.27	72.47±1.74***
Oat beverage	65.25±2.13***	**Barley**	22.71±0.71	5.52±0.82	52.55±1.07***

[a] % Removal was compared with the negative control; * represents significant differences between different food matrixes to aqueous matrixes. ***, $p \leq 0.0001$; **, $p \leq 0.001$; *, $p \leq 0.05$. Results are means of three replicated dishes.

4. Conclusion

The present work provided evidence that powdered corn by-products, corn cob in particular, could be used as a low-cost and non-toxic material for AFB_1 removal from aqueous solutions. The finding showed that, within one hour, the CCP had high % adsorption of up to 98%, and it was significantly affected by CCP dose, adsorption duration (0.25 to 8 h), particle size (<500 µm), temperature (4, 20, 37 and 50°C), but less by pH (2 to 8). The investigation of theoretical adsorption models was conducted by the adsorption kinetics, thermodynamics, and isotherms

models, which suggested that the AFB_1 adsorption on CCP was a fast and exothermic reaction, occurring with a homogeneous adsorption process. The adsorption was reversible, and could be easily desorbed by ethanol. For the first time, AFB_1 adsorption by individual cob components (cellulose, (arabino)xylan, lignin) was investigated in the present study, with lignin showing the strongest adsorption. The result suggested that the adsorption of AFB_1 on CCP not only relied on the interaction between AFB_1 molecules and cob components, but the porous cellular organization of corn cob played the most important role. On assessing the practical application, CCP showed a good decontamination ability of AFB_1 in milks and grain cleaning.

In conclusion, CCP made from corn by-products has shown strong potential as an adsorbent for aflatoxin removal which could be applied to decontaminate AFB_1 from liquid matrixes. Compare with other adsorbents for AFB_1, CCP is eco-friendly, safe, efficient, easy-operated, and no unpleasant odor or flavor is brought into the food. Nevertheless, some limitations including low specificity and the difficulty to separate after using cannot be ignored. The present study is primary research for corn cob as an AFB_1 adsorbent, so further studies need to be performed to understand the adsorption capacity of CCP to other mycotoxins, so that this adsorbent could be used in multi-mycotoxins removal in more practical food settings (e.g. fruit juice and spice extracts). Furthermore, in the practical application, the competitive adsorption of multi-compounds, including nutrients, on CCP should be considered.

Declaration of Competing Interest

The authors declare that they have no known competing financial interests or personal relationships that could have appeared to influence the work reported in this paper. CO is employed by Oatly UK. Oatly UK or any member of the Oatly Group did not influence the research design, and/or collection or interpretation of the research results. The views and opinions reflected in this manuscript do not necessarily represent the views or opinions of Oatly UK or the Oatly Group.

CRediT authorship contribution statement

Yue Liu: Investigation, Methodology, Formal analysis, Data curation, Writing, Funding acquisition, Project administration - original draft; Lei Xia: Methodology, Formal analysis, Review; Joseph Hubert Galani Yamdeu: Methodology, Review, Editing; Yunyun Gong: Study design, Supervision, Review, Editing; Caroline Orfila: Funding acquisition, Project administration, Supervision, Visualization, Review, Editing.

Acknowledgements

The authors acknowledge the technical support from Sara Viney, Dr Joanne Sier, Miles Ratcliffe, and Can Can Huang.

Funding

This project received financial support from Natural Science Foundation of Xiamen, China (3502Z202371020) to YL, the BBSRC and Innovate UK (BB/S020950/1, CitruSafe project) to CO and the BBSRC (BB/P027784/1, AFRICAP project) to JHGY, YYG and CO.

Appendix A. Supplementary data

Supplementary data to this article can be found online at

Reference

Abbas, Ali, S., Rizwan, M., Zaheer, I. E., Malik, A., Riaz, M. A., . . . Al-Wabel, M. I. (2018). A critical review of mechanisms involved in the adsorption of organic and inorganic contaminants through biochar. *Arabian Journal of Geosciences, 11*(16). doi:10.1007/s12517-018-3790-1

Abedi, E., Mousavifard, M., & Bagher Hashemi, S. M. (2022). Ultrasound-Assisted Detoxification of Ochratoxin A: Comparative Study of Cell Wall Structure, Hydrophobicity, and Toxin Binding Capacity of Single and Co-culture Lactic Acid Bacteria. *Food and Bioprocess Technology, 15*(3), 539-560. doi:10.1007/s11947-022-02767-7

Abedi, E., Pourmohammadi, K., Mousavifard, M., & Sayadi, M. (2022). Comparison between surface hydrophobicity of heated and thermosonicated cells to detoxify aflatoxin B1 by co-culture *Lactobacillus plantarum* and *Lactobacillus rhamnosus* in sourdough: Modeling studies. *LWT - Food Science and Technology, 154*, 1-14. doi:10.1016/j.lwt.2021.112616

Assaf, J. C., El Khoury, A., Atoui, A., Louka, N., & Chokr, A. (2018). A novel technique for aflatoxin M1 detoxification using chitin or treated shrimp shells: in vitro effect of physical and kinetic parameters on the binding stability. *Applied Microbiology and Biotechnology, 102*(15), 6687-6697. doi:https://doi.org/10.1007/s00253-018-9124-0

Assirey, E. A., & Altamimi, L. R. (2021). Chemical analysis of corn cob-based biochar and its role as water decontaminants. *Journal of Taibah University for Science, 15*(1), 111-121. doi:10.1080/16583655.2021.1876350

Avantaggiato, G., Greco, D., Damascelli, A., Solfrizzo, M., & Visconti, A. (2013). Assessment of multi-mycotoxin adsorption efficacy of grape pomace. *Journal of Agricultural and Food Chemistry, 62*(2), 497-507. doi:10.1021/jf404179h

Bonto, A. P., Tiozon, R. N., Jr., Sreenivasulu, N., & Camacho, D. H. (2021). Impact of ultrasonic treatment on rice starch and grain functional properties: A review. *Ultrasonics Sonochemistry, 71*, 1-13. doi:10.1016/j.ultsonch.2020.105383

Cai, Y. X., Liu, L. M., Tian, H. F., Yang, Z. N., & Luo, X. G. (2019). Adsorption and Desorption Performance and Mechanism of Tetracycline Hydrochloride by Activated Carbon-Based Adsorbents Derived from Sugar Cane Bagasse Activated with $ZnCl_2$. *Molecules, 24*(24). doi:10.3390/molecules24244534

Campagnollo, F. B., Mousavi Khaneghah, A., Borges, L. L., Bonato, M. A., Fakhri, Y., Barbalho, C. B., . . . Oliveira, C. A. F. (2020). *In vitro* and *in vivo* capacity of yeast-based products to bind to aflatoxins B_1 and M_1 in media and foodstuffs: A systematic review and meta-analysis. *Food Research International, 137*, 1-16. doi:10.1016/j.foodres.2020.109505

Choi, J. Y., Nam, J., Yun, B. Y., Kim, Y. U., & Kim, S. (2022). Utilization of corn cob, an essential agricultural residue difficult to disposal: Composite board manufactured improved thermal performance using microencapsulated PCM. *Industrial Crops and Products, 183*, 1-12. doi:10.1016/j.indcrop.2022.114931

Chukwuemeka-Okorie, H. O., Ekemezie, P. N., Akpomie, K. G., & Olikagu, C. S. (2018). Calcined Corncob-Kaolinite Combo as New Sorbent for Sequestration of Toxic Metal Ions From Polluted Aqua Media and Desorption. *Frontiers in Chemistry, 6*, 1-13. doi:10.3389/fchem.2018.00273

FAOSTATS. (2021). Food and Agriculture Organization of the United Nations. http://www.fao.org/faostat/en/#home

Galvano, F., Pietri, A., Fallico, B., Bertuzzi, T., Scire, S., Galvano, M., & Maggiore, R. (1996). Activated Carbons in Vitro Affinity for Aflatoxin B_1 and Relation of Adsorption Ability to Physicochemical Parameters. *Journal of Food Protection, 59*(5), 545-550.

Greco, D., D'Ascanio, V., Santovito, E., Logrieco, A. F., & Avantaggiato, G. (2019). Comparative efficacy of agricultural by-products in sequestering mycotoxins. *Journal of the Science of Food and Agriculture, 99*(4), 1623-1634. doi:10.1002/jsfa.9343

Guo, C., Yue, T., Hatab, S., & Yuan, Y. (2012). Ability of inactivated yeast powder to adsorb patulin from apple juice. *Journal of Food Protection, 75*(3), 585-590. doi:https://doi.org/10.4315/0362-028X.JFP-11-323

Harshitha, C. G., Sharma, N., Singh, R., Sharma, R., Gandhi, K., & Mann, B. (2022). Interaction study of aflatoxin M1 with milk proteins using ATR-FTIR. *Journal of Food Science and Technology*, 1-9. doi:10.1007/s13197-022-05587-x

Hu, Liang, W. X., Zhang, Y. Y., Wu, S. Y., Yang, Q. N., Wang, Y. B., . . . Liu, Q. J. (2018). Multipurpose Use of a Corncob Biomass for the Production of Polysaccharides and the Fabrication of a Biosorbent. *ACS Sustainable Chemistry & Engineering, 6*(3), 3830-3839. doi:10.1021/acssuschemeng.7b04179

Jääskeläinen, A. S., Holopainen-Mantila, U., Tamminen, T., & Vuorinen, T. (2013). Endosperm and aleurone cell structure in barley and wheat as studied by optical and Raman microscopy. *Journal of Cereal Science, 57*(3), 543-550. doi:10.1016/j.jcs.2013.02.007

Jawad, A. H., Mohammed, S. A., Mastuli, M. S., & Abdullah, M. F. (2018). Carbonization of corn (*Zea mays*) cob food residue by one-step activation with sulfuric acid for methylene blue adsorption. *Desalination and Water Treatment, 118*, 342-351. doi:10.5004/dwt.2018.22680

Jaynes, W. F., Zartman, R. E., & Hudnall, W. H. (2007). Aflatoxin B_1 adsorption by clays from water and corn meal. *Applied Clay Science, 36*(1-3), 197-205. doi:10.1016/j.clay.2006.06.012

Ji, Lin, H., Chen, Y. F., Dong, Y. B., & Imran, M. (2015). Corn cob modified by lauric acid and ethanediol for emulsified oil adsorption. *Journal of Central South University, 22*(6), 2096-2105. doi:10.1007/s11771-015-2734-0

Ji, & Xie, W. L. (2021). Removal of aflatoxin B_1 from contaminated peanut oils using magnetic attapulgite. *Food Chemistry, 339*, 1-8. doi:10.1016/j.foodchem.2020.128072

Karakaya, A. (2011). *Purification of Polyphenolic Compounds from Crude Olive Leaf Extract.* (Master of Science Master's thesis), İzmir Institute of Technology, Turkey. Retrieved from http://hdl.handle.net/11147/3085

Li, Y. N., Wang, R., Chen, Z. X., Zhao, X. P., Luo, X. H., Wang, L., . . . Teng, F. (2020). Preparation of magnetic mesoporous silica from rice husk for aflatoxin B1 removal: Optimum process and adsorption mechanism. *PLoS One, 15*(9), 1-18. doi:10.1371/journal.pone.0238837

Liu, Y., Benohoud, M., Galani Yamdeu, J. H., Gong, Y. Y., & Orfila, C. (2021). Green extraction of polyphenols from citrus peel by-products and their antifungal activity against *Aspergillus flavus*. *Food Chemistry: X, 12*, 1-10. doi:10.1016/j.fochx.2021.100144

Liu, Y., Galani Yamdeu, J. H., Gong, Y. Y., & Orfila, C. (2020). A review of postharvest approaches to reduce fungal and mycotoxin contamination of foods. *Comprehensive Reviews in Food Science and Food Safety*, 1-40. doi:https://doi.org/10.1111/1541-4337.12562

Ma, Cai, X. F., Mao, J., Yu, L., & Li, P. W. (2021). Adsorptive removal of aflatoxin B_1 from vegetable oils via novel adsorbents derived from a metal-organic framework. *Journal of Hazardous Materials, 412*, 1-14. doi:10.1016/j.jhazmat.2021.125170

Ojedokun, A. T., & Bello, O. S. (2017). Liquid phase adsorption of Congo red dye on functionalized corn cobs. *Journal of Dispersion Science and Technology, 38*(9), 1285-1294. doi:10.1080/01932691.2016.1234384

Palade, L. M., Dore, M. I., Marin, D. E., Rotar, M. C., & Taranu, I. (2020). Assessment of Food By-Products' Potential for Simultaneous Binding of Aflatoxin B1 and Zearalenone. *Toxins (Basel), 13*(1), 1-20. doi:10.3390/toxins13010002

Pourmohammadi, K., Sayadi, M., Abedi, E., & Mousavifard, M. (2022). Determining the adsorption capacity and stability of Aflatoxin B_1, *Ochratoxin* A, and *Zearalenon* on single and co-culture *L.*

acidophilus and *L. rhamnosus* surfaces. *Journal of Food Composition and Analysis, 110*, 1-15. doi:10.1016/j.jfca.2022.104517

Rafique, H., Dong, R., Wang, X., Alim, A., Aadil, R. M., Li, L., . . . Hu, X. (2022). Dietary-Nutraceutical Properties of Oat Protein and Peptides. *Frontiers in Nutrition, 9*, 1-14. doi:10.3389/fnut.2022.950400

Rasheed, Ain, Q. U., Yaseen, M., Santra, S., Yao, X., & Liu, B. (2020). Assessing the Aflatoxins Mitigation Efficacy of Blueberry Pomace Biosorbent in Buffer, Gastrointestinal Fluids and Model Wine. *Toxins (Basel), 12*(7), 1-21. doi:10.3390/toxins12070466

Rose, Inglett, G. E., & Liu, S. X. (2010). Utilisation of corn (*Zea mays*) bran and corn fiber in the production of food components. *Journal of the Science of Food and Agriculture, 90*(6), 915-924. doi:10.1002/jsfa.3915

Roye, C., Bulckaen, K., De Bondt, Y., Liberloo, I., Van De Walle, D., Dewettinck, K., & Courtin, C. M. (2019). Side‐by‐side comparison of composition and structural properties of wheat, rye, oat, and maize bran and their impact on in vitro fermentability. *Cereal Chemistry, 97*(1), 20-33. doi:10.1002/cche.10213

Serra, M., Weng, V., Coelhoso, I. M., Alves, V. D., & Brazinha, C. (2020). Purification of Arabinoxylans from Corn Fiber and Preparation of Bioactive Films for Food Packaging. *Membranes (Basel), 10*(5), 1-22. doi:10.3390/membranes10050095

Shar, Z. H., Fletcher, M. T., Sumbal, G. A., Sherazi, S. T., Giles, C., Bhanger, M. I., & Nizamani, S. M. (2016). Banana peel: an effective biosorbent for aflatoxins. *Food Additives & Contaminants: Part A, 33*(5), 849-860. doi:10.1080/19440049.2016.1175155

Sun, Song, A. K., Wang, B., Wang, G. F., & Zheng, S. L. (2018). Adsorption behaviors of aflatoxin B_1 and zearalenone by organo-rectorite modified with quaternary ammonium salts. *Journal of Molecular Liquids, 264*, 645-651. doi:https://doi.org/10.1016/j.molliq.2018.05.091

Zahoor, M., & Ali Khan, F. (2014). Adsorption of aflatoxin B1 on magnetic carbon nanocomposites prepared from bagasse. *Arabian Journal of Chemistry, 11*(5), 729-738. doi:10.1016/j.arabjc.2014.08.025

Zhu, Shen, D. K., & Luo, K. H. (2020). A critical review on VOCs adsorption by different porous materials: Species, mechanisms and modification methods. *Journal of Hazardous Materials, 389*(1-27), 122102. doi:10.1016/j.jhazmat.2020.122102

Zou, Fu, J., Chen, Z., & Ren, L. (2021). The effect of microstructure on mechanical properties of corn cob. *Micron, 146*, 1-7. doi:10.1016/j.micron.2021.103070

Graphical Abstract

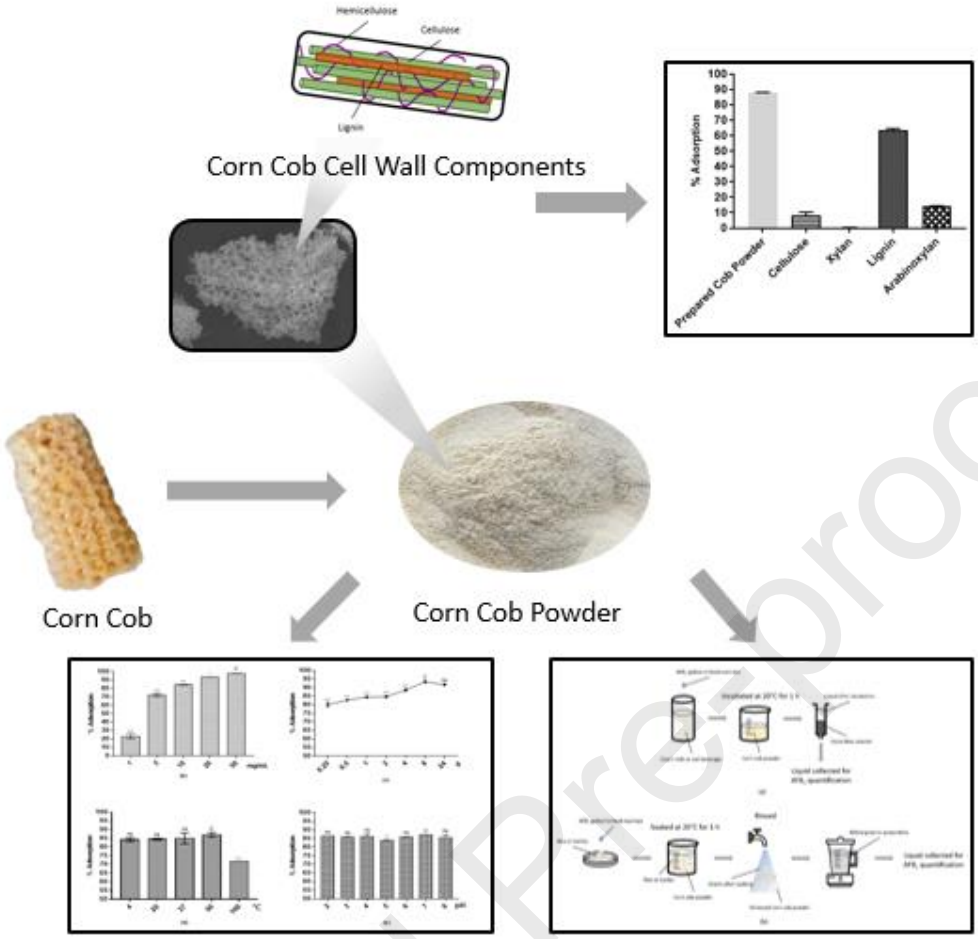

Highlights:

- Corn cob powder showed the highest AFB_1 adsorption ability among the corn by-products.
- Powder particle size, adsorbent dose, adsorption time, temperature and pH, had significant effects on adsorption.
- Cell wall components of corn cob did not individually display strong adsorption behavior.
- Corn cob powder could reduce the AFB_1 content from contaminated liquid and solid food matrixes.

The authors declare that they have no known competing financial interests or personal relationships that could have appeared to influence the work reported in this paper. CO is employed by Oatly UK. Oatly UK or any member of the Oatly Group did not influence the research design, and/or collection or interpretation of the research results. The views and opinions reflected in this manuscript do not necessarily represent the views or opinions of Oatly UK or the Oatly Group.